Materials Chemistry and Physics 151 (2015) 351–356

Contents lists available at ScienceDirect

Materials Chemistry and Physics

journal homepage: www.elsevier.com/locate/matchemphys

Shell-isolated nanoparticle-enhanced fluorescence (SHINEF) of CdTe quantum dots

Monica Ramírez-Maureira [a], Víctor Vargas C. [a], Ana Riveros [b], Paul J.G. Goulet [c], Igor O. Osorio-Román [d, *]

[a] Facultad de Ciencias, Universidad de Chile, Santiago, 7800003, Chile
[b] Facultad de Ciencias Químicas y Farmacéuticas, Universidad de Chile, Santiago, 7803287, Chile
[c] Department of Chemistry and Biomolecular Science, Clarkson University, Potsdam, NY, 13699-5810, USA
[d] Facultad de Química, Pontificia Universidad Católica de Chile, Santiago, 7820436, Chile

HIGHLIGHTS

- Shell-Isolated Nanoparticles-Enhanced Fluorescence (SHINEF).
- Synthesis of CdTe quantum dot.
- Layer-by-Layer technique for thin films preparation.
- Different size of CdTe quantum dots.
- Size effect of quantum dots in enhanced factor.

GRAPHICAL ABSTRACT

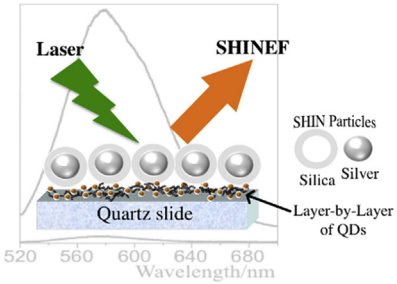

ARTICLE INFO

Article history:
Received 18 April 2014
Received in revised form
27 November 2014
Accepted 5 December 2014
Available online 11 December 2014

Keywords:
Thin films
Chemical synthesis
Coatings
Semiconductors

ABSTRACT

We report shell-isolated nanoparticle-enhanced fluorescence (SHINEF) of CdTe quantum dots. Enhanced spectra are obtained after Ag SHINs were spread onto homogenous CdTe quantum dot/polyelectrolyte layer-by-layer (LbL) films on quartz. The thin silica shell of the SHINs effectively isolates the Ag cores, preventing short-range quenching to the metal and enabling plasmon enhancement of the quantum dot fluorescence (ca. 35 fold).

1. Introduction

Hybrid structures of semiconductor and metal nanoparticles are currently of great interest and intense research. By combining the properties of these materials it is possible to obtain functional systems with applications in sensing, optoelectronics, fluorescence, bioimaging, and biosensing [1–3]. Light activates hybrid nanostructures of this type, as both QDs and plasmonic metal nanoparticles demonstrate unique optical properties when irradiated with electromagnetic radiation [1,2,4–6]. QDs typically absorb and emit light in the visible, and when compared with organic fluorophores, exhibit several important advantages including: (i)

* Corresponding author.
E-mail address: iosorior@uwindsor.ca (I.O. Osorio-Román).

http://dx.doi.org/10.1016/j.matchemphys.2014.12.003
0254-0584/

narrow emission spectra, (ii) tunable spectroscopic properties, (iii) photochemical stability, (iv) high quantum yields, and (v) the ability to generate multi-color fluorescence with a single excitation wavelength [7–9]. Metallic nanoparticles, on the other hand, are capable of confining and enhancing electromagnetic radiation, giving rise to the extremely active new research field of plasmonics [10–12]. Plasmonics relates to the nanoscale location, orientation, and manipulation of electromagnetic waves beyond the diffraction limit. This phenomenon results from the collective oscillation of conduction electrons in the metal, generating enhanced electric fields around the nanoparticles. These oscillations are commonly referred to as a localized surface plasmon resonances (LSPR) [3,10–13].

To date, several research groups have reported the fabrication of quantum dot-plasmonic nanoparticle hybrid structures [2,4–6,14–18]. Much of this work has demonstrated biological applications of enhanced QD fluorescence, where semiconductor nanoparticles have been used as sensors [6,14,18,19]. The reports agree that there is electromagnetic enhancement of QD fluorescence near plasmonic metallic nanoparticles, with maximum reported enhancement factor of ca. 20 for CdSe nanoparticles [15]. This value is comparable with the average enhancement factors that are commonly reported for the fluorescence of organic molecules.

The use of silver shell-isolated nanoparticles (Ag-SHINs), silver coated with a nanometric SiO_2 layer avoids short-range quenching to the metal surface and allowing significant enhancement of the QD emission. These nanoparticles, encapsulated in a very thin SiO_2 shell were first used for SERS applications, and that is the origin of the acronym SHINERS [20]. The use of SHINs to enhance fluorescence was subsequently demonstrated by Guerrero and Aroca, now known as SHINEF (Shell-Isolated Nanoparticles Enhanced Fluorescence) [21].

In this report, it is shown that the fluorescence emission from a thin layer-by-layer film of CdTe QDs can be enhanced by Ag SHINs. The amplification of the fluorescence is shown to be connected with the λ_{max} of the emission of the QDs. Specifically, the green emission (maximum at 526 nm) of CdTe QDs with a diameter of ~3 nm is enhanced by a maximum factor of only ca. 12, while the orange emission (maximum at 585 nm) of the CdTe QDs with a diameter of ~5 nm is enhanced by a factor of 35.

2. Material and methods

Sodium borohydride (98%), mercaptosuccinic acid (MSA) (>98%), disodium tetraborate (>98%), Trisodium citrate dihydrate (99%), silver nitrate (99.999%) and a solution of sodium silicate were purchased from Merck. Hydroxylamine hydrochloride (99%), 3-aminopropyltriethoxysilane (APTS) (>98%), Poly(2-dimethylamino)ethyl methacrylate) methyl chloride quaternary salt (MADQUAT), sodium chloride (>99.5%), cadmium chloride (99.99%) and potassium tellurite hydrate (>95%) were purchased from Sigma–Aldrich. Milli-Q grade water (>18 M) was used for aqueous solutions. All chemicals were analytical grade and used without further purification.

The synthesis of CdTe QDs is based upon protocols described previously [8,22], and on a protocol developed by our group [7]. All reactions were carried out in 50 mL of a buffer solution that contained 15 mM $Na_2B_4O_7$ and 15 mM citrate (pH = 7.5). $CdCl_2$, Na_2TeO_3 and $NaBH_4$ were added at 0.8, 0.22 and 18 mM final concentrations, respectively, and the solution was stirred vigorously for 5 min. MSA was added to the solution to reach a final concentration of 20 mM and it was kept stirring at 100 °C for 7 h after the solution reached an orange color. MSA-CdTe QDs were precipitated twice with ethanol and centrifuged for 3 min at 12,000 rpm. The supernatants were discarded and purified QDs were dried for 24 h under vacuum at room temperature. QD solutions were prepared by dissolving each of the two dried precipitates into 25 mL of milli-Q water. We call these samples CdTe-green, for the semiconductor nanoparticles that have a fluorescence maximum at 536 nm and were obtained after 2 h of synthesis, and CdTe-orange for the nanoparticles that have a fluorescence maximum at 583 nm and were obtained after 6 h. Elemental analysis of CdTe QDs was performed using energy dispersive X-ray spectroscopy (EDS), which allowed for the estimation of the concentration of nanoparticles deposited onto the quartz through layer-by-layer assembly.

The quartz surface was modified with polyelectrolyte MADQUAT 4.5 w/v % (*weight/volume percent*) and quantum dots (CdTe-MSA) following a layer-by-layer (LbL) method (More details on the experiments of layer-by-layer is given in the Supporting information). The quartz slides were sonicated, in turn, in acetone, NaOH (1 M), 1:1 (v/v) ethanol/water, and water, for about 15 min each. Electrostatic LbL assemblies (MADQUAT/QDs) were grown by alternately immersing the slides in the polycation solution (+), and the as-obtained CdTe QDs solution (−), for about 20 min each. Between each step the surface was immersed in Mili-Q water for 5 min, and dried under a nitrogen stream or under vacuum. The water used for washing was changed between each immersion. To quantify the QDs that were deposited onto the quartz slide, the samples were analyzed using inductively coupled plasma atomic emission spectroscopy (ICP-AES). The ICP-AES samples were prepared from samples with a single layer of (MADQUAT) and a single layer of QDs. These samples (quartz slide with QDs) were immersed in 5 mL of 5 M HNO_3 at 30 °C for 2 h to perform the digestion. Upon removal, the quartz slide was washed further with 5 M HNO_3 to remove any remaining of Cd and Te, with this we obtained a volume close to 10 mL. The solution was then cooled and brought to a volume of 10 mL with distilled water in a volumetric flask. This procedure was performed for 5 separate samples for each type of QD (CdTe-green and CdTe-orange).

The silver colloids were prepared via the reduction of silver nitrate with hydroxylamine, according to the method of Leopold et al. [23]. Briefly, hydroxylamine solution 1.5×10^{-3} M (45 mL) was added to the reaction flask and droplets of a 1 M NaOH solution were added to adjust the pH to a value of 10.5. Then 1 mL of $AgNO_3$ solution (1×10^{-2} M) was added dropwise to the stirring solution of NH_2OH. The mixture was stirred for 25 min at room temperature. To coat the nanoparticles, the procedure described by Wang et al. [24] was followed. The pH of 50 mL of silver nanoparticle solution was adjusted to a value of 10.5. 150 mL ethanol and 200 μL of TEOS was then added to the mixture. The mixture was stirred at room temperature for 70 min, and was then centrifuged at 11,000 rpm for 7 min to concentrate the particles with a final volume of ca. 8 mL.

3. Instruments and measurements

Atomic Force Microscopy (AFM) images were recorded using a Digital Instruments NanoScope IV, operating in tapping mode with an Al-coated n^+-silicon tip (model TESPA, Bruker AFM tips). Images were collected with high resolution (512 lines per scan) at a scan rate of 0.5 Hz. Digital processing and roughness calculations were made using the free SPM data analysis software Gwyddion 2.30. For transmission electron microscope imaging, CdTe QDs solutions were drop cast onto 400 mesh carbon-coated Cu grids. Upon solvent evaporation, images were obtained using a JEOL 2010 HR-TEM. Zeta potential and dynamic light scattering (DLS) measurements of aqueous CdTe QDs were carried out using a Zetasizer nano S90 light scattering system (Malvern Instruments Limited, UK), using a refractive index of 2.6. Absorption spectra were recorded using a

Varian Cary 50 scan UV–Vis spectrophotometer. Solution fluorescence spectra were recorded using an ISS-PC1 photon-counting spectrophotometer. The quantum yields of QD fluorescence in solution were measured by comparison with Rhodamine-B in water ($\phi_f = 0.31$), and we used the protocol reported by Grabolle at al [25].

Fluorescence spectra of the thin film samples were recorded using a Renishaw Research Raman microscope system RM 2000. This system is equipped with a Peltier charge-coupled device (CCD) detector and Leica microscope. Fluorescence spectra obtained using the 514.5 nm excitation line of an Argon-ion laser. Single-point spectra were recorded with 4 cm^{-1} resolution and 10 s accumulation times. All measurements were recorded in backscattering geometry using a 50× microscope objective with a numerical aperture value of 0.75, providing a scattering area of approximately 1 μm^2. All spectral acquisition conditions were chosen to avoid sample degradation.

4. Results and discussion

CdTe QDs were characterized using HR-TEM to determine their size (Fig. 1A). CdTe particles were found to be roughly spherical with diameters ranging between 2 nm and 3 nm (CdTe-green) and 5 nm–8 nm (CdTe-orange). Dynamic light scattering (DLS) examination of QD samples revealed that the QDs have average sizes of 3.2 and 5.4 nm for CdTe-green and CdTe-orange, respectively (Fig. 1B). Additionally, the QD Z-potential values were found to be −17.9 mV and −18.5 mV for CdTe-green and CdTe-orange, respectively. Sizes determined for the as-prepared CdTe QDs were similar to those produced by other authors [5,8,9,22,26].

The absorption and fluorescence spectra for these two QD samples are shown on Fig. 1C and D, and agree with those previously reported for CdTe nanocrystals [7,8,22,26]. Fluorescence with maxima around 536 nm (CdTe-green) and 583 nm (CdTe-orange) is observed (Fig. 1D and Table 1). As expected, the absorbance and fluorescence emission of the larger nanocrystals (CdTe-orange) is redshifted relative to the smaller diameter particles (CdTe-green). The physical reason is the quantum confinement effect. The fluorescence is directly related to the energy levels of the quantum dot. Quantitatively, the bandgap energy that determines the energy (and hence color) of the fluorescent light is inversely proportional to the size of the quantum dot. Larger quantum dots have more energy levels, and are more closely spaced between each. This allows the quantum dot to absorb photons containing less energy, i.e., those closer to the red end of the spectrum [27–29].

Furthermore, as shown in Fig. 1D, the fluorescence spectrum of CdTe-orange has a value full width at half maximum (FWHM) more higher than the spectrum of CdTe-green (see Table 1), indicating that the particle size distribution of the CdTe QDs increases with synthesis time. This result is confirmed by the DLS data, where we

Table 1
CdTe QDs fluorescence spectral range, peak maximum and full width at half maximum (FWHM).

Samples	Emission (nm)	Maximum (nm)	FWHM
CdTe-green	450–620	526	43
CdTe-orange	500–700	585	62

Table 2
EDS elemental analysis of CdTe NPs.

% Element	Samples	
	CdTe-green	CdTe-orange
C	32.89	31.47
O	30.63	29.07
Na	4.56	2.00
S	15.31	14.35
Cd	9.94	17.13
Te	6.58	5.99

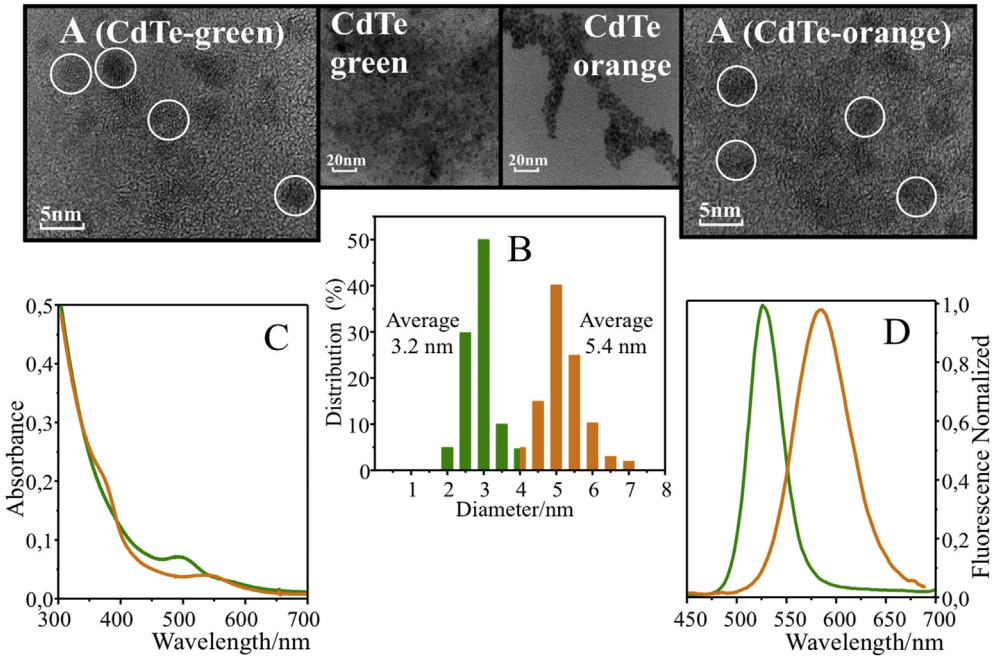

Fig. 1. Characterization of CdTe QDs. On top are shown images of high-resolution transmission electron microscopy (HR-TEM), on a scale of 20 nm and a scale of 5 nm. On the center (Fig. 1B) are shown the results obtained by dynamic light scattering (DLS) (The green bars and orange bars correspond to CdTe-green and to CdTe-orange, respectively). Finally on bottom, Fig. 1C and D are shows the absorption and fluorescence spectra of CdTe QDs (The spectra in green line and orange line correspond to CdTe-green and CdTe-orange, respectively). (For interpretation of the references to color in this figure legend, the reader is referred to the web version of this article.)

observed a larger size distribution for the CdTe-orange sample (see Fig. 1B).

Quantum yields (ϕ) were evaluated to determine fluorescence efficiency. CdTe QDs displayed ϕ values of 0.15 and 0.48 for CdTe-green and CdTe-orange, respectively. These results are in agreement with those reported for other thiol-capped CdTe QDs [8,22,26].

Energy dispersive X-ray spectroscopy (EDS) elemental analysis showed that the CdTe QDs are composed of cadmium, tellurium, as well as carbon, sulfur, oxygen, and sodium (Table 2). Interestingly, the percentage of Te was nearly constant in all of the samples (~6%), while the percentage of Cd increased with NP size (Table 2). This could result from thermal decomposition, and loss from the nanocrystal surface, of mercaptosuccinic acid (MSA), thus favoring the deposition of a CdS layer on CdTe nanoparticles. In this context, most of CdTe QDs described to date have been shown to have a CdS layer on their surface. Red colored CdTe nanocrystals show increased Cd/Te ratios and less carbon and oxygen content, suggesting the formation of a CdS layer on larger CdTe QDs [7,8].

Fig. 2 shows the AFM characterization of the QD thin films produced in this work using the LbL technique. For these samples, calculations of root mean square roughness (Rq) and roughness average (Ra) were performed. The 3 images on the top of the figure correspond to a scans of 5 × 5 μm^2, and the bottom 3 images are of 1 × 1 μm^2 scans. From a review of the images in Fig. 2, it can be concluded that the polymer and the QDs were both effectively transferred to the quartz substrate, and that there are slight differences between the morphologies of CdTe-green and CdTe-orange samples. This is confirmed by the values of Rq and Ra, which increase when compared with the data obtained for quartz (see Table 3). This indicates that the layer-by-layer technique allows good transfer of polymer and the QDs to the surface of the quartz slide, which is in agreement with previous publications [30–32].

Fig. 3 shows the absorption and fluorescence spectra of the thin films of CdTe-green and CdTe-orange. The absorption spectra show bands at 490 nm (CdTe-green) and 548 nm (CdTe-orange), in agreement with the data from solution. This indicates that the transfer of the nanoparticles from solution to the thin film does not significantly alter the photophysical properties of the CdTe QDs. Furthermore, fluorescence spectra were recorded from different points of the sample (fifty spectra on each surface) and the spectra that are shown in Fig. 3B correspond to the average. Maxima were

Table 3
Analysis of roughness of the thin film.

Sample	Root mean square roughness (nm)	Roughness average (nm)
Quartz	0.28	0.21
CdTe-green	0.57	0.44
CdTe-orange	0.72	0.54

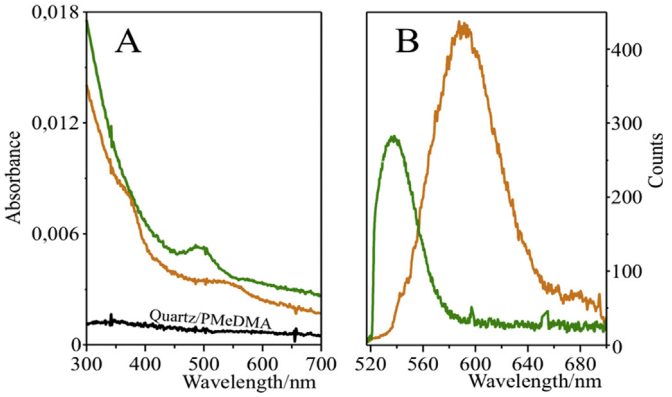

Fig. 3. Absorption (A) and fluorescence (B) spectra of the thin films CdTe QDs. The spectra with green continuous line and orange continuous line correspond to CdTe-green and to CdTe-orange, respectively. Finally, on bottom of Fig. 3A we show the baseline of the absorption spectra, it was subtracted from the absorption spectra of the QDs. (For interpretation of the references to color in this figure legend, the reader is referred to the web version of this article.)

observed at 536 nm and 583 nm, for CdTe-green and CdTe-orange samples, respectively. The fluorescence intensity was higher for CdTe-orange due to its higher quantum yield (Fig. 3B). These results are in agreement with the values obtained for samples in solution.

A single layer of CdTe QDs was assembled onto a quartz slide to measure the enhanced fluorescence produced by silver SHINs. The quantity of QDs assembled onto the film was estimated using inductively coupled plasma atomic emission spectroscopy (ICP-AES) data. For this estimate, values from Table 2, QD diameters from dynamic light scattering, and the mass of Cd^{2+} determined by ICP-AES on a quartz surface of 2.5 cm^2, were used along with the ionic radius of Cd^{2+} [33]. For the estimate of the quantity of

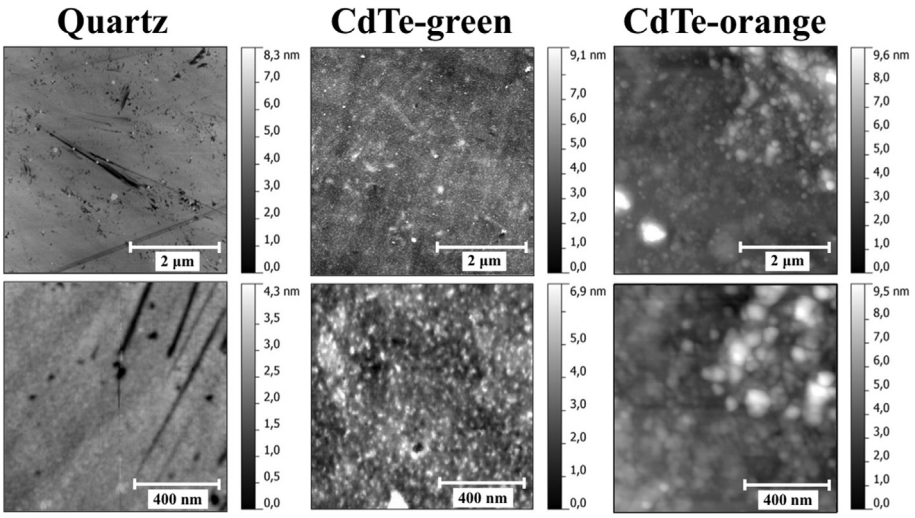

Fig. 2. Atomic force microscopy (AFM) of the surfaces fabricated through layer-by-layer technique. The images correspond correspondence to a scanning of 5 x 5 microns, and at the bottom a zoom of 1 x 1 microns.

nanoparticles, the values of Te^{2-} were not used because the process of digestion in acid medium performed for ICP-AES could produce volatile hydrotellurites or telluric acid, causing the values measured in solution to be unreliable. Cadmium values are reliable, however, since the Cd^{2+} ion is stable in solution.

The estimated number of QDs in the thin film sample is higher for CdTe-green than for CdTe-orange (see Table 4). This is due to the fact that the number of particles required to cover a given area is larger for small particles than it is for large particles (Details of the calculation in Supporting information, Fig. S5).

To measure enhanced fluorescence of CdTe Quantum Dots, silver nanostructures coated with a nanometric layer of SiO_2 (Ag SHINs) were deposited onto the thin films of CdTe-green and CdTe-orange. The LSPR spectra of the silver nanoparticles before and after SiO_2 coating are shown in Fig. 4. HR-TEM images of the Ag-SHINs are also included as insets in Fig. 4. The redshift of the extinction peak from 400 to 415 nm is consistent with a changed dielectric medium due to silica coating, as predicted by the theory [34]. The TEM images show 30–60 nm diameter particles that deviate slightly from spherical shape. The particles are clearly coated with silica and the coating is fairly homogenous, with a shell thickness of approximately 8–12 nm on average. To perform the SHINEF experiments, a drop of the SHIN particles (3 μL) was deposited onto the thin films (on the quartz slide) and allowed to dry. A 2D spatial mapping of a small surface area yielded enhancement factors for the integrated intensity of the emission in the range of 8–10 for CdTe-green and the range of 30–40 for CdTe-orange. The surface-enhanced fluorescence spectra shown in Fig. 5A and B correspond to average SEF enhancement over the probed surface for CdTe-green and CdTe-orange, respectively. The spectra with the lowest fluorescence intensity (dashed lines) correspond to reference average spectra of a layer of CdTe QDs without Ag-SHINs. This result confirms that there is a distribution of enhancement factors (EF) that contribute to the observed enhanced signal, and that some localized spots may have a fairly large enhancement factor compared to the observed average. To illustrate this, several SHINEF spectra for CdTe-green and CdTe-Orange are shown in Fig. 5C and D, respectively.

The results in Fig. 5 reveal a difference in the magnitude of the enhancement of the fluorescence for CdTe-green and CdTe-orange. Since the SHINEF experiments have been carried out by casting the Ag–SHIN, the formation of aggregates on the surface may lead to red shifted plasmons providing electromagnetic enhancement with an uneven distribution on the surface, and in favor of the CdTe-orange [35,36]. Finally, Fig. 5C and D also reveal a minor change in the shape of the spectrum of CdTe-orange, or spectral profile modification introduced by the plasmon enhancement [35,37]. The reference fluorescence spectrum of CdTe-orange on quartz has only one maximum (583 nm), while the amplified spectrum shows a maximum at 580 nm, and in some spectra shoulders around 608 and 660 nm are detected.

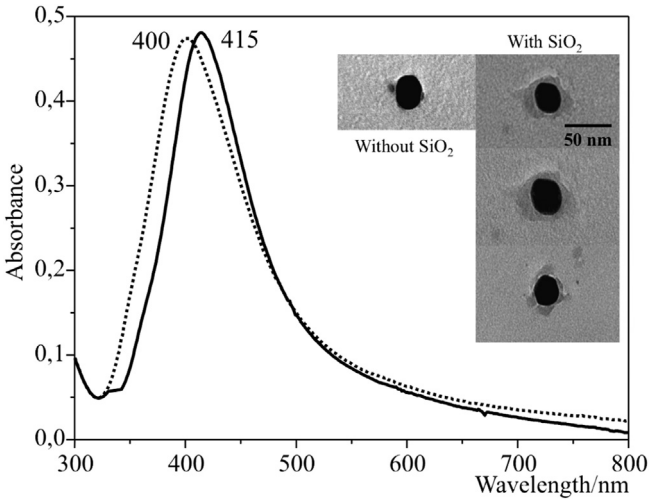

Fig. 4. Absorption spectra of the silver particles before coating (dashed line) (λ max = 400 nm) and after coating (continuous line) (λ max = 415 nm). Inset: high-resolution transmission electron microscopy (HR-TEM) images of the coated particles. The bar in the images represents 50 nm.

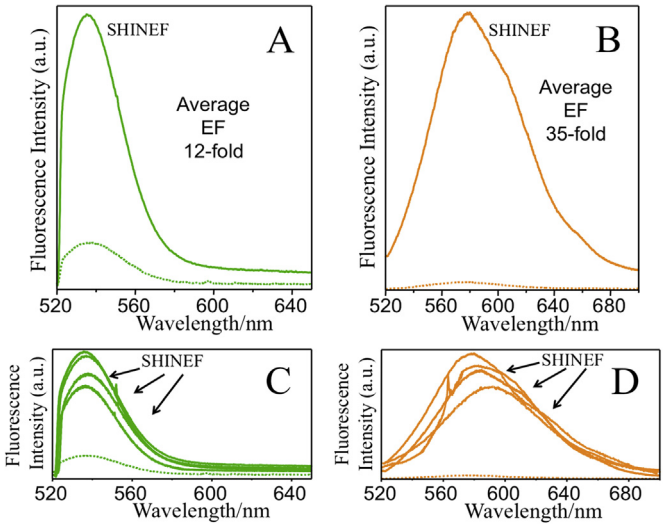

Fig. 5. SHINEF of CdTe QDs. Fig. 5A and B and corresponds to an average SEF enhancement over the probed surface for CdTe-green and CdTe-orange, respectively. Enhancement factors of the emission are in the range of 8–10 for CdTe-green and range of 30–40 for CdTe-orange, with average values of 12-fold and 35-fold, respectively. Fig. 5C and D are shown spectral profile modification of enhancement factors that contribute to the observed enhanced signal for CdTe-green and CdTe-orange, respectively. Finally, for this figure all the spectra with dashed line correspond to average spectra of CdTe QDs without SHINs. (For interpretation of the references to color in this figure legend, the reader is referred to the web version of this article.)

Table 4
Estimate of the amount of CdTe QDs in a layer on quartz.

Samples	ICP-AES (Cd^{2+}/T^{2-}) in mg[a]	Diameter of QDs[b] (nm)	Nanoparticle volume (nm^3)[c]	N° of QDs[d] per μm^2
CdTe-green	1.25/0.46	3.0	14.14	3.95×10^6
CdTe-orange	0.53/nd	5.0	65.45	2.88×10^5

nd: not detected.

[a] The limit detection of instrument is 0.005 mg and 0.01 mg for Cd^{2+} and Te^{2-}, respectively.

[b] Corresponds to an average, the values reported in the table were calculated from the HR-TEM and dynamic light scattering results.

[c] Volume of a sphere $V = 4/3\pi r^3$, where $\pi = 3.1416$ and r = radius.

[d] The mass in mg determined by ICP-AES, these values were converted to moles and then a number of nanoparticles through the Avogadro number.

5. Conclusion

Silver shell-isolated nanoparticle-enhanced fluorescence (SHINEF) of CdTe quantum dot/polyelectrolyte layer-by-layer films is reported. We demonstrated the fabrication of relatively homogenous films was obtained that allowed the observation of SHINEF of CdTe nanocrystals, where the emission enhancement factors were 10-fold and 35-fold for CdTe-green and CdTe-orange, respectively. In this sense, it was observed that enhancement is different for CdTe-green and CdTe-orange, we could to propose that the

formation of aggregates on the surface may lead to red shifted plasmons providing electromagnetic enhancement with an uneven distribution on the surface, and in favor of the CdTe-orange.

In summary, develop films that mix quantum dots and shell-isolated nanoparticles, could have applications in different fields of materials science.

Acknowledgment

Authors acknowledge the financial support of FONDECYT. A.R. to Grand N^0 1130425 and postdoctoral grand N^0 3130654 and I.O.O-R. to initiation research grant N^0 11100067. M.R-M. acknowledges to CONICYT scholarships for PhD study in Chile N^0 21120624. P.J.G.G. gratefully acknowledges Clarkson University for startup funding. Finally, I.O.O-R acknowledges Dr. Ricardo Aroca for valuable advice and discussion.

Appendix A. Supplementary data

Supplementary data related to this article can be found at http://dx.doi.org/10.1016/j.matchemphys.2014.12.003.

References

[1] W. Zhuyuan, Z. Shenfei, L. Wang, W. Chunlei, X. Shuhong, C. Hui, C. Yiping, J. Am. Chem. Soc. 134 (2012) 2993–3000.
[2] P. Yang, K. Kawasaki, M. Ando, N. Murase, J. Nanopart. Res. 14 (2012) 1025–1036.
[3] M.B. Cortie, A.M. McDonagh, Chem. Rev. 111 (2011) 3713–3735.
[4] R.D. Artuso, G.W. Bryant, A. Garcia-Etxarri, J. Aizpurua, Phys. Rev. B 83 (2011) 235406–235415.
[5] L.M. An, Y.Q. Yang, W.H. Su, J. Yi, C.X. Liu, K.F. Chao, Q.H. Zeng, J. Nanosci. Nanotechnol. 10 (2010) 2099–2103.
[6] V. Biju, T. Itoh, A. Anas, A. Sujith, M. Ishikawa, Anal. Bioanal. Chem. 391 (2008) 2469–2495.
[7] V. Díaz, M. Ramírez-Maureira, J.P. Monrás, J. Vargas, D. Bravo, I.O. Osorio-Román, C.C. Vásquez, J.M. Pérez-Donoso, Sci. Adv. Mater. 4 (2012) 609–616.
[8] E. Ying, D. Li, S. Guo, S. Dong, J. Wang, PLoS One 3 (2008) e2222, 1–8.
[9] K. Qasim, W. Lei, Q. Li, J. Nanosci. Nanotechnol. 13 (2013) 3173–3185.
[10] R.F. Aroca, Phys. Chem. Chem. Phys. 15 (2013) 5355–5363.
[11] M. Rycenga, C.M. Cobley, Z. Jie, L. Weiyang, C.H. Moran, Z. Qiang, Q. Dong, X. Younan, Chem. Rev. 111 (2011) 3669–3712.
[12] K.M. Mayer, J.H. Hafner, Chem. Rev. 111 (2011) 3828–3857.
[13] M. Moskovits, Rev. Mod. Phys. 57 (1985) 783–826.
[14] C. Xiang, L. Mei, L. Baoxin, Analyst 137 (2012) 3293–3299.
[15] E. Cohen-Hoshen, G.W. Bryant, I. Pinkas, J. Sperling, I. Bar-Joseph, Nano Lett. 12 (2012) 4260–4264.
[16] K. Munechika, Y. Chen, A.F. Tillack, A.P. Kulkarni, I. Jen-La Plante, A.M. Munro, D.S. Ginger, Nano Lett. 11 (2011) 2725–2730.
[17] Y. Matsumoto, R. Kanemoto, T. Itoh, S. Nakanishi, M. Ishikawa, V. Biju, J. Phys. Chem. C 112 (2008) 1345–1350.
[18] P. Mulvaney, L.M. Liz-Marzán, M. Giersig, T. Ung, J. Mater. Chem. 10 (2000) 1259–1270.
[19] M. Haridas, J.K. Basu, D.J. Gosztola, G.P. Wiederrecht, Appl. Phys. Lett. 97 (2010) 083307–083309.
[20] J.F. Li, Y.F. Huang, Y. Ding, Z.L. Yang, S.B. Li, X.S. Zhou, F.R. Fan, W. Zhang, Z.Y. Zhou, D.Y. Wu, B. Ren, Z.L. Wang, Z.Q. Tian, Nature 464 (2010) 392–395.
[21] A. Guerrero, R.F. Aroca, Angew. Chem. Int. Ed. 50 (2011) 665–668.
[22] N. Gaponik, D.V. Talapin, A.L. Rogach, K. Hoppe, E.V. Shevchenko, A. Kornowski, A. Eychmüller, H. Weller, J. Phys. Chem. B 106 (2002) 7177–7185.
[23] N. Leopold, B. Lendl, J. Phys. Chem. B 107 (2003) 5723–5727.
[24] J.X. Wang, J.S. Buckley, J.L. Creek, J. Dispers. Sci. Tech. 25 (2004) 287–298.
[25] M. Grabolle, M. Spieles, V. Lesnyak, N. Gaponik, A. Eychmuller, U. Resch-Genger, Anal. Chem. 81 (2009) 6285–6294.
[26] W.W. Yu, L. Qu, W. Guo, X. Peng, Chem. Mater. 15 (2003) 2854–2860.
[27] A.I. Ekimov, A.L. Efros, A.A. Onushchenko, Solid State Comm. 56 (1985) 921–924.
[28] H.M. Schmidt, H. Weller, Chem. Phys. Lett. 129 (1986) 615–618.
[29] A.F. van Driel, G. Allan, C. Delerue, P. Lodahl, W.L. Vos, D. Vanmaekelbergh, Phys. Rev. Lett. 95 (2005) 236804.
[30] S. Srivastava, N.A. Kotov, Layer-by-Layer (LBL) assembly with semiconductor nanoparticles and nanowires, in: A. Rogach (Ed.), Semiconductor Nanocrystal Quantum Dots; Synthesis, Assembly, Spectroscopy and Applications, Springer, New York, 2008, pp. 197–216.
[31] S. Ishii, R. Ueji, S. Nakanishi, Y. Yoshida, H. Nagata, T. Itoh, M. Ishikawa, V. Biju, J. Photochem. Photobiol. A 183 (2006) 285–291.
[32] N.A. Kotov, I. Dekany, J.H. Fendler, J. Phys. Chem. 99 (1995) 13065–13069.
[33] D.R. Lide (Ed.), CRC Handbook of Chemistry and Physics, 89th ed., 2008-2009. New York.
[34] T.R. Jensen, M.L. Duval, K.L. Kelly, A.A. Lazarides, G.C. Schatz, R.P. Van Duyne, J. Phys. Chem. B 103 (1999) 9846–9853.
[35] R.F. Aroca, G.Y. Teo, H. Mohan, A.R. Guerrero, P. Albella, F. Moreno, J. Phys. Chem. C 115 (2011) 20419–20424.
[36] Y. Zhang, A. Dragan, C.D. Geddes, J. Phys. Chem. C 113 (2009) 12095–12100.
[37] R. Gillz, E.C. Le Ru, Phys. Chem. Chem. Phys. 13 (2011) 16366–16372.